Sustainable Cities and Society 68 (2021) 102786

Contents lists available at ScienceDirect

Sustainable Cities and Society

journal homepage: www.elsevier.com/locate/scs

Assessment of urban flood vulnerability using the social-ecological-technological systems framework in six US cities

Heejun Chang [a,*], Arun Pallathadka [a], Jason Sauer [b], Nancy B. Grimm [b], Rae Zimmerman [c], Chingwen Cheng [d], David M. Iwaniec [e], Yeowon Kim [f,g], Robert Lloyd [e], Timon McPhearson [g,h,i], Bernice Rosenzweig [j], Tiffany Troxler [k], Claire Welty [l], Ryan Brenner [c], Pablo Herreros-Cantis [g]

[a] Department of Geography, Portland State University, Portland, OR, 97201, USA
[b] School of Life Sciences, Arizona State University, Tempe, AZ, 85287, USA
[c] Wagner Graduate School of Public Service, New York University, New York, NY, 10012, USA
[d] The Design School, Arizona State University, Tempe, AZ, 85287, USA
[e] Urban Studies Institute, Georgia State University, Atlanta, GA, 30303, USA
[f] Global Institute of Sustainability and Innovation, Tempe, AZ, 85281, USA
[g] Urban Systems Lab, The New School, New York, NY, 10003, USA
[h] Cary Institute of Ecosystem Studies, Millbrook, NY, 12545, USA
[i] Stockholm Resilience Centre, Stockholm University, Stockholm, Sweden
[j] Environmental Science, Sarah Lawrence College, Bronxville, NY, 10708, USA
[k] Earth and Environment Department and Sea Level Solutions Center in the Institute of Environment, Florida International University, Miami, FL, 33199, USA
[l] Department of Chemical, Biochemical, and Environmental Engineering and Center for Urban Environmental Research and Education, University of Maryland, Baltimore County, Baltimore, MD, 21250, USA

ARTICLE INFO

Keywords:
Urban flood
Vulnerability
Social-ecological-technological systems
Resilience
Mapping

ABSTRACT

As urban populations continue to grow through the 21st century, more people are projected to be at risk of exposure to climate change-induced extreme events. To investigate the complexity of urban floods, this study applied an interlinked social-ecological-technological systems (SETS) vulnerability framework by developing an urban flood vulnerability index for six US cities. Indicators were selected to reflect and illustrate exposure, sensitivity, and adaptive capacity to flooding for each of the three domains of SETS. We quantified 18 indicators and normalized them by the cities' 500-yr floodplain area at the census block group level. Clusters of flood vulnerable areas were identified differently by each SETS domain, and some areas were vulnerable to floods in more than one domain. Results are provided to support decision-making for reducing risks to flooding, by considering social, ecological, and technological vulnerability as well as hotspots where multiple sources of vulnerability coexist. The spatially explicit urban SETS flood vulnerability framework can be transferred to other regions facing challenging urban floods and other types of environmental hazards. Mapping SETS flood vulnerability helps to reveal intersections of complex SETS interactions and inform policy-making for building more resilient cities in the face of extreme events and climate change impacts.

1. Introduction

Flooding is a major form of hazard that affects millions of people worldwide. According to the OECD (2016), global flood damage exceeds $40 billion annually. Together with growing populations in flood-prone areas, climate change and rising sea levels are projected to increase the number of people vulnerable to flood disasters to two billion people by 2050 (UNESCO World Water Assessment Programme, 2012). Because many cities are located in river floodplains or along the coast, urban areas are frequently exposed to floods; approximately $^1/_8$ of urban land in the United States is located in high-risk flood zones, affecting nearly a quarter-million people living in those zones (Qiang, Lam, Cai, & Zou, 2017). Flood damages in the United States have costed nearly $17 billion per year between 2010 and 2018 (ASFPM, 2020). With increases in frequency and intensity of precipitation driven by climate change (Kunkel et al., 2020), flood zones are likely to expand by 40–45 % by the

* Corresponding author.
E-mail address: changh@pdx.edu (H. Chang).

https://doi.org/10.1016/j.scs.2021.102786
Received 20 October 2020; Received in revised form 5 January 2021; Accepted 14 February 2021

end of the 21st century (American Rivers, 2020). Nevertheless, drainage patterns and flood-mitigation infrastructure in most cities are not designed to adapt to the anticipated climate change-induced urban flooding hazards, thus posing potential technological risk to cities (Gimenez-Maranges, Pappalardo, La Rosa, Breuste, & Hof, 2020; Mohtar, Abdullah, Maulud, & Muhammad, 2020; Rosenzweig et al., 2018). It is this city level that emerges as a critical geographic level for understanding and mitigating flood hazards. Moreover, integrating the multiple domains of social, ecological and technological concerns is critical at the urban scale.

Following the IPCC's vulnerability conceptual framework (McCarthy et al., 2001), which separately considers exposure (the extent to which an entity experiences a hazard, usually based on location and timing), sensitivity (how much the entity is likely to be affected if exposed to the hazard, as a consequence of internal characteristics), and adaptive capacity (the potential for an entity to adjust when influenced by a hazard, thus reducing impact), many studies have conducted flood vulnerability assessments at national (Khajehei, Ahmadalipour, Shao, & Moradkhani, 2020) and regional (Cheng, 2019a) scales. However, only a few studies have investigated intra-city-level flood vulnerability (Gu et al., 2018), despite heterogeneous distributions of people and nature within the city. Previous studies show socially and economically disadvantaged groups tend to be particularly exposed to flood hazards in urban areas (Collins, Grineski, Chakraborty, & Flores, 2019). For example, after Hurricane Harvey, people with disabilities were disproportionately affected by flooding (Chakraborty, Grineski, & Collins, 2019).

Flood vulnerability assessment is a vital tool for flood mitigation (Nasiri, Yusof, & Ali, 2016), as municipal governments strive to reduce potential damages resulting from anticipated extreme events. An indicator approach to flood vulnerability assessment has been frequently adopted in the past decade (Table 1). Following pioneering research conducted by Müller, Reiter, and Weiland (2011), who developed indicators across multiple scales, many studies used a combination of social, physical, and environmental indicator variables (Erena & Worku, 2019; Salazar-Briones, Ruiz-Gibert, Lomelí-Banda, & Mungaray-Moctezuma, 2020). They used widely available geospatial data and/or interview data to select or weigh appropriate indicators, showing spatial variation in flood vulnerability at the urban scale. For example, Nasiri, Yusof, Ali, and Hussein (2019) developed a district-level flood vulnerability index comprising 25 indicators that encompass social, economic, environmental, and physical components in Kuala Lumpur City, Malaysia. Based on experts' opinions, they eventually selected 10 indicators, identifying different components of vulnerability indicators that are disproportionately associated with district-level flood vulnerability within the city. However, these studies did not examine ecological or technological vulnerability explicitly. Kim, Eisenberg, and Bondank (2017) suggested the importance of urban flood vulnerability assessment by combining social and technological system domains, while jointly assessing the traffic load on roadways and hydrologic capacity of stormwater drainage in Phoenix, USA. Borrowing from concepts of landscape ecology, Han et al. (2020) found that an increasing number of small patch sizes and leapfrogging and edge-expanding types of development were positively correlated to flood occurrence. Ferrari, Oliveira, Pautasso, and Zêzere (2019) further extended the previous approach by using 59 indicators in two European cities and reported high local variability in flood vulnerability, which is undetectable from national- or continental-scale data. Ferrari et al.'s study also showed that urban inequalities are related to disparities in flood vulnerability.

While some previous studies included environmental indicators in vulnerability analysis as reported in Table 1, these studies did not sufficiently examine such indicators in relation to S and T domains collectively. Moreover, environmental indicators typically have focused on hydrometeorological and topographic indicators, rather than ecological ones as the current paper does. In fact, assessments are seldom performed across all domains – social, ecological and technological - that are potentially at risk from flooding: i.e., the people, natural systems, and the infrastructure built by cities to support their way of life. Most previous flood vulnerability studies examined social vulnerability (Cutter, Boruff, & Shirley, 2003) or social and physical vulnerability (Cho & Chang, 2017).

We consider cities and urban regions as dynamic social-ecological-technological systems (SETS) (Grimm, Pickett, Hale, & Cadenasso, 2017; McPhearson et al., 2016; Markolf et al., 2018), that experience flooding both within and across SETS domains, and that capture interactions among the components. Thus, a more holistic approach is needed to assess flood vulnerability of complex urban SETS and to improve planning that builds resilience in SETS domains (Cheng, Yang, Ryan, Yu, & Brabec, 2017). The integration of S, E, and T with exposure, sensitivity and adaptability is an innovative addition to urban sustainability. The social dimension directly addresses society. The applicability to six cities underscores its relevance to cities and transferability to other cities. Sustainable development addresses convergence of environment, economy, and equity, which requires understanding of complex systems and the interconnected components. SETS provides a framework to examine the complex relationship between environment, infrastructure, and equity to advance understanding of the context for impacts and response to distribution of hazards in society.

Additionally, these earlier studies mostly focused on one or two cities (with the exception of Sterzel et al., 2020), and few, if any, have addressed the ecological domain of flood vulnerability (Römer et al., 2012; Weißhuhn, Müller, & Wiggering, 2018). By ecological

Table 1
Representative indicator-based studies on empirical urban flood vulnerability that used indicators mapped to social, ecological, and technological domains.

Authors	Study region	Social vulnerability indicators	Ecological vulnerability indicators	Technological vulnerability indicators
Adelekan (2011)	Abeokuta, Nigeria	Gender, age, education, income, occupation, past flood experience, risk perception, length of residence	N/A	Building structure
Müller et al. (2011)	Santiago, Chile	Age, gender, education, household size, employment status, experience, knowledge	Green space per building block	Constructional materials, position of building, flood protection infrastructure,
Erena and Worku (2019)	Dire Dawa City, Ethiopia	Population, population density, early warning, past experience, age >65, gender, education, family size, insurance, communication, cultural heritage, access to sanitation, industries	Slope	Building materials, emergency service, dikes-levees, evacuation route
Salazar-Briones et al. (2020)	Mexicali, Baja California, Mexico	Age <14 and > 60, unemployed, replying on medical service, education, household infra	Slope, proximity to inundation area topographic wetness index, land use & soil type, sub-basin flow	N/A
Nasiri et al. (2019)	Kuala Lumpur, Malaysia	Population density, flood experience	Rainfall amount, # of river, open land	Proportion of low cost buildings, Length of drainage system
Sterzel et al. (2020)	Coastal cities worldwide	Population, urban expansion, income, slum population	Wetland, cyclone, flood occurrence	N/A

vulnerability, we refer to an ecosystem's inability to cope with or adjust in response to floods, in contrast to technological vulnerability, which we define as infrastructure's diminished capacity to recover and adapt to floods. Thus, we seek to fill the gap in the literature by using the SETS framework. The SETS approach has been recently used in cross-comparative flood risk management (Chang et al., 2021), co-developing scenario visions of urban resilience and sustainability (Iwaniec, Cook, Davidson, Berbés-Blázquez, Georgescu et al., 2020, b),

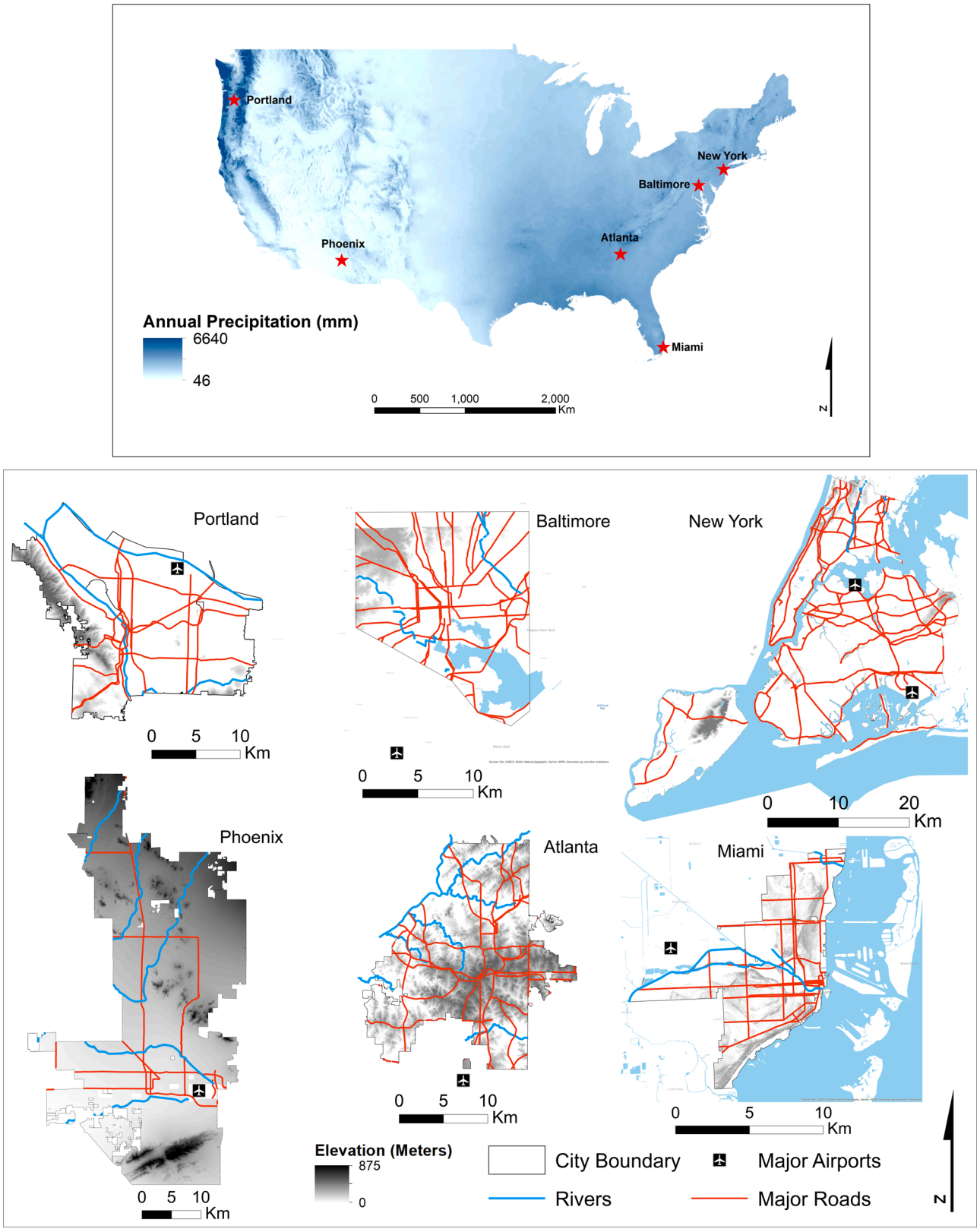

Fig. 1. Relative location of six study cities in the United States with average annual precipitation (1981-2010) as background and major roads and waterways in each city with elevation as background.

constructing a climate justicescape (Cheng, 2019b), and reviewing nature-based solutions for flood resilience (Keeler et al., 2019). Here, we undertook a comparative study of SETS vulnerability across six cities to answer the following research questions:

(1) What are the spatial patterns of urban flood vulnerability when using social (S), ecological (E), and technological (T) indicators separately? Which of these factors and their combination explain the spatial variation of flood vulnerability?
(2) To what degree do the vulnerable areas identified by each of S, E, and T indicators spatially correlate with each other?
(3) How are the vulnerability indicators clustered together to explain the combined SETS flood vulnerability across the study cities?
(4) What are the added values of investigating flood vulnerability using a SETS framework so that it can potentially be applied to other areas? How does the SETS framework reveal the hidden dimensions of flood vulnerability?

2. Study area

The study areas consist of six US cities – Atlanta, Baltimore, Miami, New York, Phoenix, and Portland – that vary in their geographical, climatic, and hydrologic characteristics (Fig. 1, Table 2). These cities encompass different climate and urbanization gradients, with population density ranging from dispersed (~1000 people/km^2 in Atlanta and Phoenix) to compact (>10,000 people/km^2 in New York City). All cities have experienced major floods in past decades, and most have experienced increasing precipitation intensity in more recent years (Cooley & Chang, 2020). Documented changes in extreme precipitation are more pronounced for the Northeast and Midwest than for other regions (Janssen, Wuebbles, Kunkel, Olsen, & Goodman, 2014), but all regions are expected to show increases under future climate change (Swain et al., 2020). Additionally, we have been studying these cities as part of the Urban Resilience to Extremes Sustainability Research Network (UREx SRN), with the goal of promoting knowledge co-production with city practitioners for climate change adaptation (Muñoz-Erickson, Miller, & Miller, 2017; Iwaniec, Cook, Davidson, Berbés-Blázquez, Georgescu et al., 2020; Cook et al. 2021). Social equity and environmental justice issues, as they relate to extreme weather-induced hazards, including floods, are a growing concern in our study cities (e.g., Fahy, Brenneman, Chang, & Shandas, 2019 and Cheng, 2019b). Lastly, and critically, data availability for a cross-city comparison study was a key component for delineating the study areas.

3. Data and methods

3.1. SETS vulnerability framework

The SETS vulnerability framework (Fig. 2) combines three dimensions of vulnerability—exposure, sensitivity, adaptive capacity—within each of the three domains of SETS: social, ecological, and technological systems that comprise urban areas. We define the vulnerability dimensions following the well-established literature (Kasperson & Kasperson, 2001, McCarthy et al., 2001, Turner et al., 2003, Polsky, Neff, & Yarnal, 2007). Our explicit point is that there are S, E, and T domains for each of the exposure, sensitivity, and adaptability dimensions. The goal is not to make assessments more complex, but rather to account for the complexity inherent to each domain of SETS in urban contexts by providing a structure for it, and thereby enable researchers to have a flexible framework that can be adapted to their needs. First, as shown in Fig. 2, there are nine SETS urban flood vulnerability realms: Social, ecological, and technological domains within each of the three vulnerability dimensions, i.e., exposure, sensitivity and adaptive capacity. Second, we selected two representative indicators in each of the nine SETS urban flood vulnerability realms in light of data availability and the need to maintain consistency in the metrics across the cities (as identified in Table 3). Social vulnerability indicators represent demography (age, language proficiency), neighborhood (population density), and socioeconomic characteristics (income, percentage renter) (Rufat, Tate, Burton, & Maroof, 2015, Kirby et al., 2019). Ecological vulnerability indicators represent land-surface characteristics (slope, land cover), landscape quality (proximity to hazard, fragmentation), and greenness (wetland, productivity). Technological vulnerability indicators represent built infrastructure (transportation, green infrastructure), public facilities (critical infrastructure, roads, emergency centers), and buildings. These indicators were carefully chosen based on a review of the literature (Table 3) and in-depth discussion among the authors based on commonalities, feasibility, and data availability for a cross-city comparison. Additionally, we identified indicators that offer spatially detailed information appropriate for use at the census block group scale. As a result, indicators that are only available at the city or regional scale were excluded in our analysis.

The purpose of this study is to expand and contribute to flood vulnerability assessments by introducing the three domains of SETS and identify where they intersect and are either synergistic or antagonistic. The indicators chosen in this study are not meant to be comprehensive; thus, we may be limited to accounting for a factor that is particularly important in one city but not all six cities. While some indicators may not be easy to classify across the three vulnerability dimensions (e.g., green infrastructure can be either T or E (Childers et al., 2019), we assigned each indicator to only one dominant vulnerability dimension to avoid double counting. However, this study aims to provide, by using the SETS framework, the methodology for selecting vulnerability indicators that can be applied at different spatial scales or to study areas that have specific attributes (for example, vulnerability to coastal flooding).

3.2. Data

Flood hazard area delineation was obtained from the Federal Management Agency (FEMA)'s 500-AA flooding (FEMA, 2020). We included all census block groups within the 500-year floodplain. Although the 100-year floodplain is more commonly used for municipal regulatory planning purposes, using 500-year floodplain maps has a couple of advantages. First, recent studies (Blessing, Sebastian, & Brody, 2017; Highfield, Norman, & Brody, 2013) point out that the current FEMA 100-year maps are inaccurate, potentially underestimating flood-prone areas in the current climate. Second, with increasing precipitation intensity under climate change scenarios, it is reasonable to assume that flood hazard zones will expand in the future. For each census block

Table 2
Selected geographic, climatic, and hydrological characteristics in the study areas of six cities in the United States.

	Portland	Phoenix	Baltimore	Atlanta	New York City	Miami
Climate (Mean annual precipitation, annual temperature range)	915 mm annual prcp. 7.8 - 17.2 °C	211 mm annual prcp. 17.2 - 30.6 °C	1034 mm annual prcp. 10 - 18.9 °C	1263 mm annual prcp. 11.7 - 22.2 °C	1174 mm annual prcp. 8.9 - 16.7 °C	1572 mm annual prcp. 21.1–28.9 °C
Population (2016)	656,097	1,611,990	605,597	474,560	8,461,961	455,973
Population density (2016)	1784/km^2	1083/km^2	2863/km^2	1082/km^2	10,807/km^2	3303/km^2
Impervious surface areas (%) (2016)	56 %	52 %	55 %	40 %	78 %	58 %

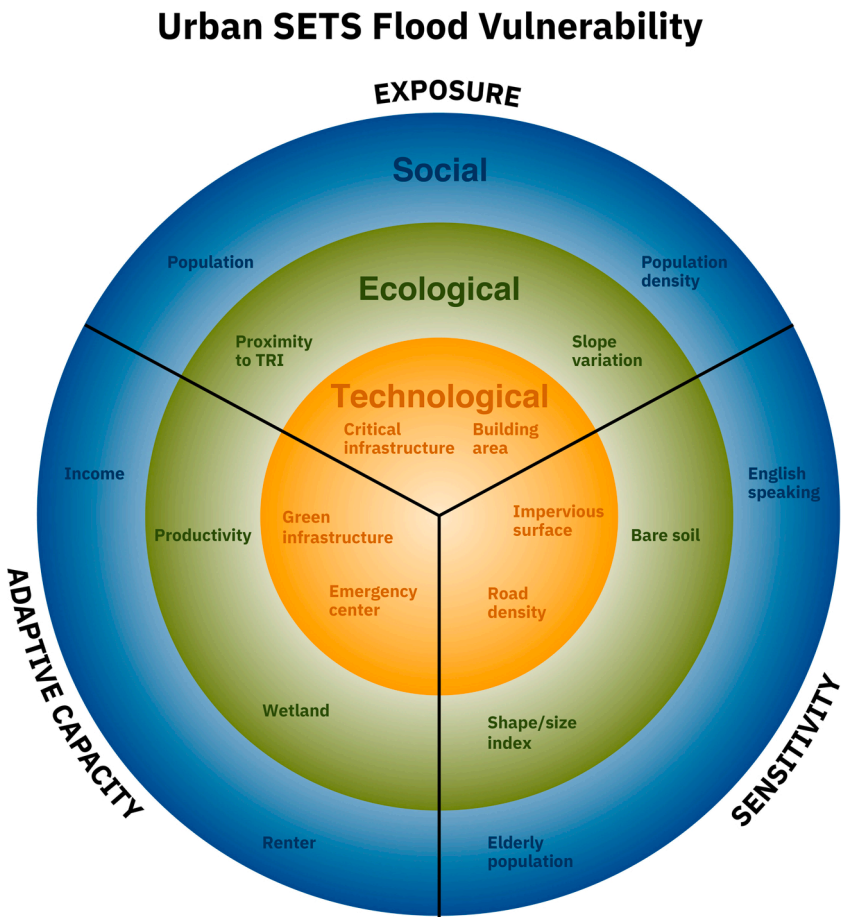

Fig. 2. The urban SETS flood vulnerability framework including selected exposure, sensitivity, and adaptive capacity indicators in each of the three SETS domains: social, ecological, and technological.

group, we obtained data from multiple agencies to compute the socio-demographic, ecological and infrastructure indicators (Table 3). These data either were already organized at the scale of the census block group or were prepared in ArcGIS 10.7 (ESRI 2020) so that they could be appropriately used at that scale.

3.3. Methods

3.3.1. Indicator construction and vulnerability score

Given that census block group size differs substantially in each city, the raw data were converted or standardized to either % or density by dividing by census block group population or area. The converted indicator values were then standardized between 0 and 1 using the minimum-maximum rescaling formula below (for exposure and sensitivity indicators) (Iyengar and Sudarshan, 1982).

$$V_i = \frac{X_i - X_{imin}}{X_{imax} - X_{imin}}$$

Where V_i = normalized value of indicator X_i, X_{imin}, and X_{imax} represent the minimum and maximum values of a specific indicator i, respectively.

For indicators that are inversely related to urban flood vulnerability, the following formula was used for standardization (e.g., higher language proficiency reduces vulnerability).

$$V_i = \frac{X_{imax} - X_i}{X_{imax} - X_{imin}}$$

We then used these normalized values to estimate urban flood vulnerability using the following formula.

$$V_s = \frac{Ex_1 + Ex_2 + St_1 + St_2}{Ad_1 + Ad_2}$$

Ex_1 = exposure indicator 1, Ex_2 = Exposure indicator 2, St_1 = sensitivity indicator 1, St_2 = sensitivity indicator 2, Ad_1 = adaptive capacity indicator 1, Ad_2 = adaptive capacity indicator 2

The final composite vulnerability score (Vs) is then normalized again to have a range between 0 and 1 (0 = the least vulnerable, 1 = most vulnerable).

3.3.2. Geospatial analysis

We used ArcGIS 10.7 to combine each indicator layer to produce social, ecological, and vulnerability maps. The vulnerability scores were mapped by quartile. We overlaid all possible permutations of individual S, E, and T top quartile flood vulnerability maps to identify which census block groups were vulnerable in one or more domains of SETS. In other words, we categorized the vulnerable areas into seven classes (i.e., S, E, T, S-E, S-T, E-T, S-E-T) and mapped the classes.

3.3.3. Statistical analysis

We used global Moran's I to identify if the spatial patterns of flood vulnerability were clustered, dispersed, or random in ArcGIS 10.7. Moran's I value close to zero indicates random spatial distribution, while positive and negative values indicate clustering (similar neighborhoods are next to each other) or dispersed (dissimilar neighborhoods are next to each other) spatial patterns, respectively (Moran, 1950). Pearson's correlation coefficients were used to examine the direction and strength of the relationship between pairs of S, E, and T for each city.

We conducted a principal component analysis (PCA) to derive major

Table 3
The selected SETS flood vulnerability indicators, their sources, and justifications of selection.

Category	Indicator	Source	Justification (hypothesized relationship)	References
Social exposure	People (total number of people on floodplain)	ACS 2016	(+) More people living in a place, more people are exposed to floods	Rufat et al. (2015), Erena and Worku (2019)
	Population density (# of people /area)	ACS 2016	(+) Densely populated areas are more vulnerable to floods	Cutter et al. (2003), Cutter (2016)
Social sensitivity	English proficiency (% English speaking people)	ACS 2016	(-) English speaking people understand flood information better	Cutter et al. (2003); Cutter (2016); Borden, Schmidtlein, Emrich, Piegorsch, and Cutter (2007); Foster et al. (2019)
	Age (% population over 65 years)	ACS 2016	(+) Older people are less mobile, need more assistance during floods	Cutter et al. (2003); Cutter (2016); Borden et al. (2007); Foster et al. (2019)
Social adaptive capacity	Median income (Household median income)	ACS 2016	(+) Higher income people have more means to cope with floods	Rufat et al. (2015), Gu et al. (2018)
	Renter (% people who are renters)	ACS 2016	(-) Renters have fewer resources to cope with floods	Ma and Smith (2020); Manturuk, Lindblad, and Quercia (2010); Gu et al. (2018)
Ecological exposure	*Standard deviation of slope (-)	High Resolution DEM from each city	(-) Higher slope variation could lower water velocity and reduce erodibility/erosion and water quality degradation	Pratt and Chang (2012)
	Proximity of ecosystem (park, floodplain) to Toxic Release Inventory (TRI) and Superfund sites	Environmental Protection Agency (EPA)	(-) Closer to hazards sites can have higher probability of contaminant release	Kiaghadi and Rifai (2019)
Ecological sensitivity	Combination of shape index and average patch size	Derived from city vegetation layers	(+) Sites with higher shape index (meaning less square shape) and smaller size patches are more sensitive to flood damage	Askins (1995); Bevers and Flather (1999); Martínez-Morales (2005); Ewers and Didham (2007)
	% bare soil within the area	NLCD 2016	(+) Bare soils are more erodible leading to higher sedimentation	Zong and Chen (2000)
Ecological adaptive capacity	*% wetland within the area	National Wetlands Inventory (NWI)	(+) Wetlands absorb flood water as added benefits	Chan et al. (2018)
	Productivity (+) based on Normalized Difference in Vegetation Index (NDVI)	USGS Global Visualization Viewer (GloVis) (2016−2017)	(+) Wetland and forest ecosystems with higher resource availability (and higher productivity) are able to resist disturbance and/or rebound more quickly	Danielson et al. (2017), Wilson et al. (2019)
Technological exposure	Building area (% building area within the area)	LiDAR/Shapefile from each city GIS department	(+) Buildings that are exposed to floods	Laudan, Rözer, Sieg, Vogel, and Thieken (2017), ten Veldhuis, Clemens, and Gelder (2011)
	Critical infrastructure (CI) (# of CI (water/wastewater, power plant, gas terminal) in the area)	Energy Information Administration (EIA)	(+) Critical infrastructure that are exposed to floods	Wilbanks and Fernandez (2014); Guidotti et al. (2016)
Technological sensitivity	Road density (Total lengths of roads/area)	Each city's GIS department	(+) Higher volume of traffic is sensitive to floods	Pregnolato, Ford, Glenis, Wilkinson, and Dawson (2017), Kim et al. (2017)
	Impervious surface (% impervious surface from high resolution)	NLCD IMPERVIOUS 2016	(+) Impervious surface area increase direct runoff	Palla and Gnecco (2015)
Technological adaptive capacity	*Green Infrastructure (GI) density (Total # GI/area)	Each city GIS and environmental protection departments	(+) GI retain rainwater and reduces peak flow	Fahy and Chang (2019)
	Emergency centers (distance of emergency centers (e.g., hospitals, schools, community centers to centroid of CBG)	City offices of emergency management	(-) Emergency centers provide assistance to the community during floods	Cutter et al. (2003)

ACS = American Community Survey; NLCD = National Land Cover Data.
* Standard deviation of the slope is included as an exposure indicator in the E domain because it represents a structural property of landscape that leads to water pooling. We intentionally differentiate constructed wetlands or green infrastructure (in the technological adaptive capacity domain) from natural wetlands (in the ecological adaptive capacity domain) so natural wetlands can fall into the E domain and the other engineered structures fall into the T domain.

components that capture most variation in the chosen indicators across all six study cities (Jolliffe, 2002). The varimax with Kaiser normalization rotation method was used for creating a rotated component matrix (Kaiser, 1958). The absolute values of the correlation coefficient between individual indicators and each component higher than 0.4 (and statistically significant) were used to select each component's indicator variables. The saved components were then used as predictors in regressions for explaining variation of combined flood vulnerability across all six cities.

4. Results

4.1. Social vulnerability map

In Portland, the highly vulnerable areas are located north and central downtown along the Willamette River and a neighborhood north of Johnson Creek in Southeast Portland (Fig. 3). With high population density, the downtown areas have a high proportion of renters and aged people, even though median income is relatively high. Neighborhoods in the Johnson Creek area have low median income and high percentage renters, with a high percentage of non-English speaking people relative to other Portland neighborhoods. In contrast, with higher income, lower percentage renters, and predominantly English-speaking people living

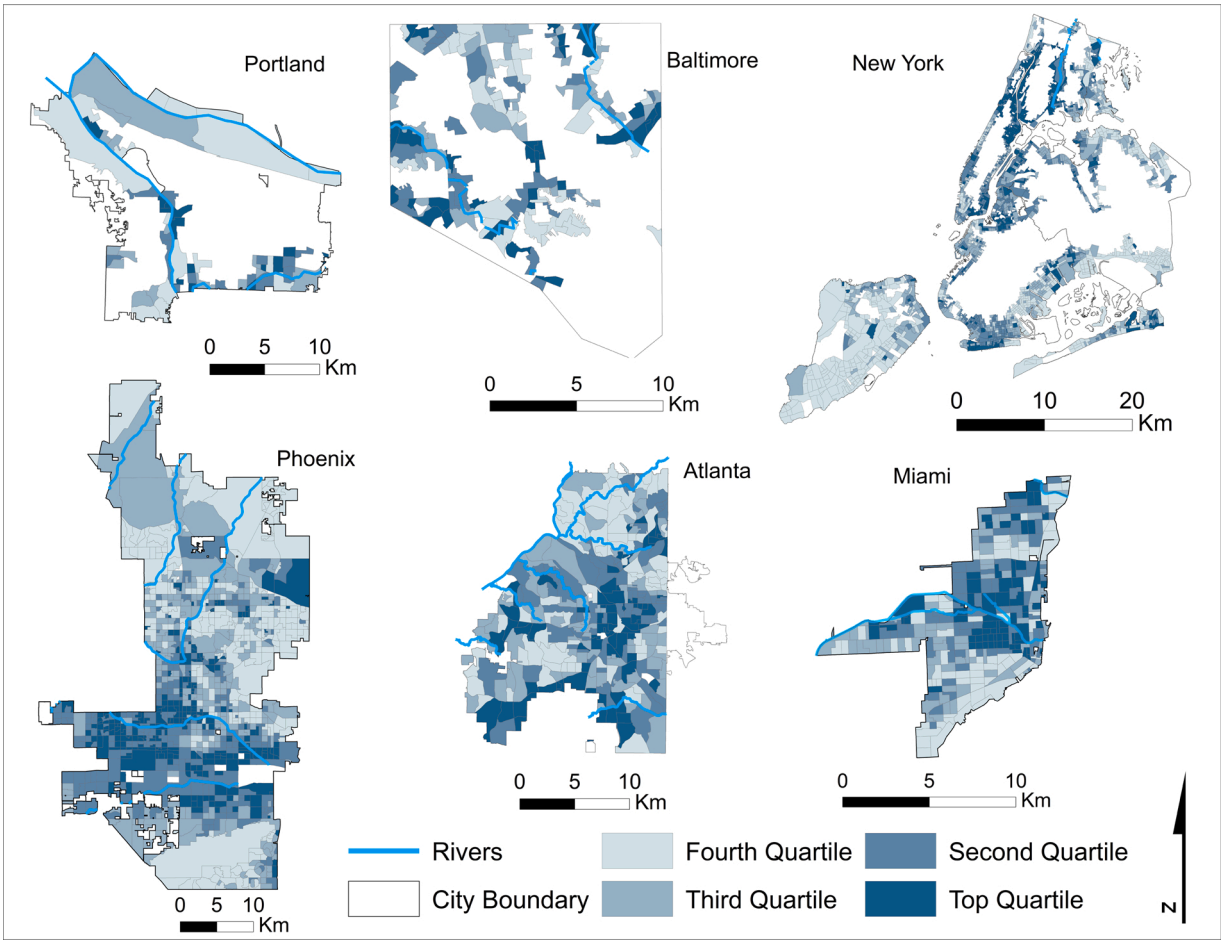

Fig. 3. Quartile maps showing census block group-scale social vulnerability to flooding for six US cities.

in low-density neighborhoods, southwest and northwest Portland have relatively low social vulnerability.

In Phoenix, the entire city is within the 500-year floodplain. Socially vulnerable areas are located primarily along both sides of the east-west interstate highway (I-10) and near the airport (Figs. 1–3), and in a west-side community north of I-10. These areas are characterized by low median income and low percentage English speakers; the latter has a high percentage of renters. A legacy of discriminatory housing practices in South Mountain Village (south of I-10) has concentrated these more socially vulnerable populations in these areas. One additional census block group in northeast Phoenix has high social vulnerability. This area is among the larger, newer census block groups in the north, and has a high percentage of renters and low median household income, but is dominated by young English-speakers, in contrast to the two southern/western areas of high vulnerability. Thus, low income, low percentage English-speaking, and high percentage renters contribute most to the pattern of high social vulnerability. Interestingly, older residents ($\geq$65 years of age) are concentrated in areas near preserves that tend to be wealthier.

In Baltimore, areas with the highest social vulnerability indicator score are located in more dense communities in general (Fig. 3). These communities also have a higher percentage of renters and lower median income. They include areas in downtown Baltimore, Fredrick Avenue, and neighborhoods along Gwynns Falls west of the city, where streams were covered for low-income apartment housing development. Other socially vulnerable areas include east Baltimore, where several major highways (I-95, I-895, 40) intersect with Herring Run. Those areas have higher population density, lower median income, lower percentage English-speaking people, and higher percentage renters than the rest of Baltimore.

In Atlanta, the entire city is in the 500-year floodplain. Within the city, many of the more socially vulnerable areas are low-income, but even some higher-income areas feature moderate to high levels of social vulnerability, due to population age in some areas and percentage renters in other areas. Higher population density (central sections) and the large numbers of people (in east and south-east sections) contributed to increased social vulnerability scores in several census block groups. Overall, English proficiency is highly variable among the vulnerable areas; however, low English proficiency in low-income areas contributed to some of the highest social vulnerability scores in the city.

In New York City, very high population densities drive social vulnerability outcomes (Fig. 3). For example, areas such as the Lower East Side are denser than the city average. In terms of social sensitivity, several areas have low English proficiency, such as the South Bronx where portions in flood-prone areas also have high proportions of Spanish-speaking populations. Financial vulnerability is an important consideration, and coastal areas of Brooklyn exemplify elderly populations with lower incomes on average. Social adaptive capacity is reflected in the high percentage renters in New York City in general. Many of them live in coastal areas vulnerable to flooding, such as in Canarsie in Brooklyn. Median income is highly variable in the vulnerable areas. Some of these areas have lower incomes, for example, the Lower East Side of Manhattan, East Harlem, and the South Bronx.

In Miami, social vulnerability is highest in parts of neighborhoods in central Miami along the Miami River and the Little River (Fig. 3). Social vulnerability is also higher in parts of neighborhoods farther away from these low-lying riverside areas (former wetland transverse glades). Other pockets exist on the east side of the city. Given that there is not

much variation in percentage English speaking across the city, the spatial pattern of social vulnerability is best defined by higher population number and density, higher percentage renters, and lower median income level in some areas around the Miami and Little Rivers, and apparently opposite patterns of percentages elderly and English-speaking. High median income seems to offset percentage elderly, contributing to relatively low social vulnerability in the coastal census block groups.

4.2. Ecological vulnerability map

The ecological dimension introduces a substantially different element from environmental characteristics, since the latter focuses on issues such as air and water quality whereas the former is concerned holistically with communities of living organisms and their relationship to environmental factors. In Portland, the most ecologically vulnerable areas are located in the northwestern tip of the city, where the Willamette and the Columbia Rivers join (Fig. 4). The areas are characterized as disturbed wetlands with a low amount of vegetation, and are near superfund sites. Other highly vulnerable areas include the northern section of Johnson Creek, which runs through the southern part of the city from east to west. Extensive industrial and commercial activities with little or fragmented vegetation make the Johnson Creek area ecologically vulnerable. In contrast, with higher productivity, large patch size, and higher slope variation, the southwestern neighborhoods have relatively low ecological vulnerability.

In Phoenix, high ecological vulnerability is concentrated in highly urbanized areas, again near the interstate highways and airport, whereas the low-vulnerability areas are the desert and mountain preserves in the northern, central, and southern parts of the city where large ecosystem patches have greater adaptive capacity. In contrast, patches in densely populated urban areas are smaller and more isolated, and thus more susceptible to damage. Even though all of Phoenix is in the 500-year floodplain, the areas of high ecological vulnerability around the river and the Grand Canal (east-west "rivers" shown in Fig. 4) are extremely flat, have extensive bare soil, and are in close proximity to TRI sites. Proximity to TRI sites also contributes strongly to the high vulnerability along the I-17 corridor (running north-south in the west; Fig. 1). Wetlands, concentrated along rivers and canals, do not contribute much to altering the pattern of ecological vulnerability.

In Baltimore, areas with the highest ecological vulnerability score are located in the downtown core of the city and highly urbanized areas adjacent to the harbor, where greenspace is fragmented into smaller urban parks with fewer wetlands, and where slope variation is low (Fig. 4). TRI sites are also concentrated near downtown areas. Additionally, ecologically vulnerable areas are found in east Baltimore, where multiple highways intersect with Herring Run. This area is relatively flat and is close to TRI sites. In contrast, parks adjacent to the floodplain in less densely developed neighborhoods of the city (i.e., the northern part of the city) tend to be larger, contiguous green spaces, making them less ecologically vulnerable.

In Atlanta, high ecological vulnerability often occurs around industrial, semi-industrial, and post-industrial sites of low ecological productivity, and near TRI sites, such as by the Chattahoochee River and the railyard in the northwest, and scattered through the southeast (Fig. 4). Intensive urbanization, larger shape index and smaller patch size, and lower productivity contribute to vulnerability in the urban cores (i.e., downtown, Midtown, and Buckhead). Elsewhere, the vegetated Atlanta

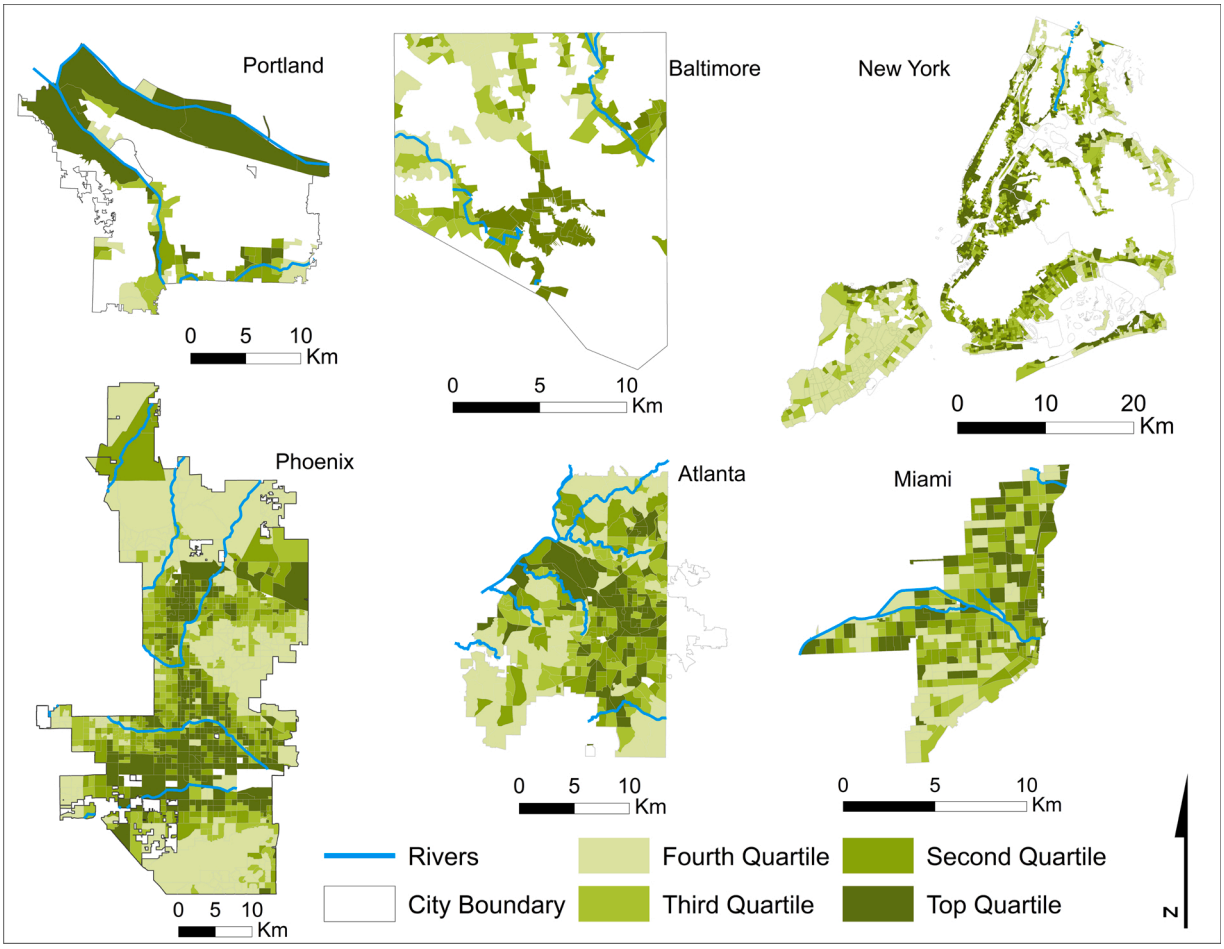

Fig. 4. Quartile maps showing census block group-scale ecological vulnerability to flooding for six US cities.

suburbs reduce vulnerability. In northern, central-eastern, and southwestern areas, the proximity of large ecosystem patches (preserves and wooded areas) along floodwater sources reduces ecological vulnerability. Wetlands are rare throughout the city but do help mitigate vulnerability near the rivers and creeks.

In New York City, the distribution of ecological vulnerability is moderated by different indicators across the studied area. For instance, in areas such as Jamaica Bay, vulnerability is high due to the low deviation in the slope values, which reflect a flat, constant topography that increases exposure, and fragmented habitat as reflected in the shape index and patch-size variable (Fig. 4). Specific industrial and post-industrial areas in the city such as Newtown Creek, Wall Street and the coast of the Hudson River show considerable ecological vulnerability due to the presence of polluted sites recorded in EPA Superfund and the TRI. Finally, the distribution of wetlands is the main vulnerability driver in the outer census block groups of the coastline, most notably in the Rockaways Peninsula, Coney Island, and the shores of Northern Queens and Southeast Bronx.

In Miami, empty lots in downtown likely contribute to the high percentage of bare soils, which likely contributes to sediment loading of waterways, increasing ecological vulnerability. A clear spatial pattern of percentage wetlands exists, with many wetlands concentrated along waterways and the coast (Fig. 4). Given the value of waterfront property and development pressure, this suggests high vulnerability of coastal areas lacking wetland conservation. Interestingly, only a subset of these wetland areas has relatively high productivity. The lower ecological vulnerability in the south part of the city seems to be driven by higher percentage wetland and productivity, larger green areas or with lower edge to area, farther distance from TRI, and lower percentage bare soils.

4.3. Technological vulnerability map

In Portland, the highly technologically vulnerable areas are located in the northeastern corner and central downtown areas (Fig. 5). The central downtown areas have a high density of buildings and critical infrastructure, serving as gas terminal hub. The northeastern corner, where the airport is located, has a high percentage impervious surface. The relatively low vulnerability in southeastern and southwestern areas is attributed to a high presence of green spaces with permeable surfaces.

In Phoenix, primary drivers of technological vulnerability are associated with the indicators that are closely related to urbanized land uses (Fig. 5). In particular, combined effects of both exposure and sensitivity indicators such as percentage building area, road density, and percentage impervious surface largely contribute to the top quartile of technological vulnerability in the broader Phoenix downtown area as well as along the busy highways (i.e., I-10 and I-17 crossing the city from east to west and from south to north, respectively). Other peripheral areas of the city (i.e., northwestern and southwestern edges) also appear vulnerable because these areas deliver less technological adaptive capacity due to limited availability of green infrastructure systems and/or emergency centers.

In Baltimore, the areas with the highest technological vulnerability score are located in the city's downtown area (Fig. 5), where there is dense commercial development and many hospital campuses with high

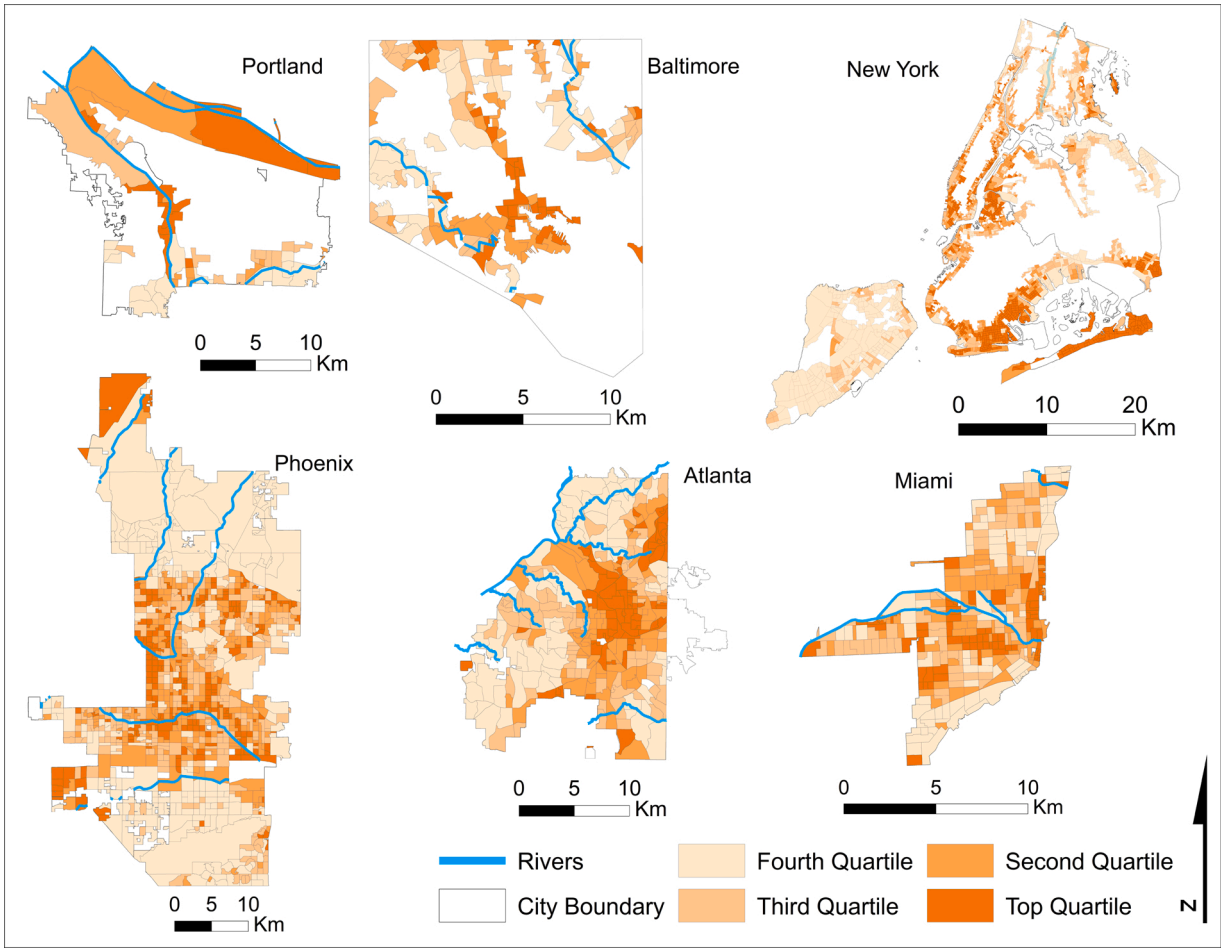

Fig. 5. Quartile maps showing census block group scale technological vulnerability to flooding for six US cities.

impervious surface area and low green infrastructure density. Industrial communities adjacent to Baltimore Harbor in the southwest of the city, with high percentages impervious surface and low green infrastructure density, were also identified as being technologically vulnerable.

In Atlanta, technological vulnerability concentrates in the heavily urbanized areas—particularly the three urban cores of downtown, Midtown, and Buckhead—and along the major highways (Fig. 5). Road density and impervious surfaces are contributing factors throughout the city, especially near the highways. Other infrastructural areas, including a railyard, also contribute to vulnerability. Hotspots (top quartile of technological vulnerability) also occur in residential areas near downtown. Higher green infrastructure density provides technological adaptive capacity in the northern and central-eastern regions of Atlanta.

In New York City, technological exposure is reflected in the traditional, historical coastal locations of many water, electric, and communication utilities, and sensitivity occurs in terms of the generally dense road networks and impervious surfaces throughout New York City, including in flood-prone vulnerable areas (Fig. 5). Technology adaptive capacity is exemplified by green infrastructure and its potential for absorbing floodwaters and primarily filtering to support water quality. Emergency centers, of which there are over 60 designated ones (and others included in emergencies) (Zimmerman, Restrepo, Joseph, & Llopis, 2017), are by definition not located in floodplains for protection, however, many vulnerable areas rely upon rapid connectivity to such facilities.

Redevelopment east of downtown and in north Miami, as well as open space in areas along the Miami River and some coasts, contribute to lower technological exposure there (Fig. 5), with the notable exception of downtown and Brickell neighborhoods. Technological vulnerability seems to be related to higher green infrastructure density and lower impervious surface cover and street density, and higher building density in other areas south of the Miami River.

4.4. Spatial autocorrelation of SETS flood vulnerability maps

Moran's I values indicate weak spatial autocorrelations in most vulnerability maps (Table 4). S, E, and T maps are all positively spatially correlated in Phoenix, Baltimore, Atlanta, and New York City, showing clustered patterns. The degree of clustering is generally higher in social and ecological vulnerability maps than in technological vulnerability maps, except for Portland. In Portland, both social and ecological vulnerability maps are randomly distributed, while the technological vulnerability map shows a high degree of clustering ($I = 0.78$). In contrast, technological vulnerability is randomly distributed in Miami, with clustering in social and ecological vulnerability.

4.5. Correlation between S, E, T maps in each city

At least one pair of vulnerability scores (i.e., between S and E or S and T or E and T) is significantly correlated for all cities except Miami (Table 5); however, correlations are weak ($0.05 < r < 0.42$, $p < 0.05$). In New York City, both S-T and E-T pairs are significantly related to each other, although they are also weakly correlated. In Phoenix and Atlanta, social and ecological indicators are weakly correlated to each other, whereas in Portland, social and technological indicators are moderately correlated.

4.6. S- E-T vulnerability map

In Portland, the S-E combined vulnerability area is found in southeast Portland, north of Johnson Creek (Fig. 6). Two census block groups—one in northeast Portland along the Columbia River where the airport is located and the other in southwest Portland along the Willamette River—show high vulnerability by E and T. Two census block groups along the Willamette River are vulnerable for all SETS domains. These areas are characterized by high presence of industrial lands with low income, little vegetation, and close proximity to TRI sites along the river.

The pattern of combined S-E vulnerability in Phoenix (Fig. 6) is clustered along the interstate highways (east-west I-10, north-south I-17, and diagonal I-60), and in the three areas of high social vulnerability, the west-side community north of I-10 (Maryvale), South Mountain Village south of the Salt River, and the new, low-income, renter community in the northeast, reflecting the legacy of past restrictive and redlining policies. There are few census block groups with overlapping S-T or S- E-T vulnerability, but those that show this combined vulnerability all are associated with the interstate highway corridors.

In Baltimore, vulnerability is primarily dominated by social factors, except for the highly industrialized communities in the coastal floodplain adjacent to the harbor, which is dominated by ecological and ecotechnical vulnerability (Fig. 6). These communities are characterized by dense urban development, including critical facilities such as hospitals, and the few remaining greenspaces are highly fragmented. A couple of communities in south and east Baltimore are vulnerable both socially and ecologically, and are close to TRI sites and highways.

In Atlanta, areas of vulnerability often cluster around the highways and other major infrastructural features (Fig. 6). Combined vulnerability areas are most prominent around downtown, where development co-locates many of the factors likely to exacerbate flooding as well as exposing sensitive populations and locations to risk. Some other combined vulnerability areas occur near the airport (Fig. 1; south of the main contiguous city boundary, but with influence extended to nearby areas, some of which are in the city limits), near the railyard west of Midtown, and in some areas of development concentrated along the highways.

In New York City, connectivity and compound effects occur for social, ecological and technological exposure, sensitivity, and adaptive capacity. The southeastern portion of the city around Jamaica Bay, which is heavily flood-prone, illustrates the confluence of SETS characteristics (Fig. 6). Exposure occurs as high population densities (S), high slope variation (E), and numerous utilities and wastewater treatment plants surrounding the Bay (T). Sensitivity occurs as high percentage elderly populations (S), irregular and fragmented patches (E), and relatively high road densities and impervious surfaces (T). Mixed adaptive capacity is reflected in higher renter populations but higher income populations in the Rockaways (S), extensive wetlands (E), and the presence of green infrastructure (T) but long distances to emergency centers given the Bay's configuration.

In Miami, domains of urban flood vulnerability are not strongly

Table 4
Moran's I values for social, ecological, technological vulnerability domains for each of six study cities.

Vulnerability Domains	Portland	Phoenix	Baltimore	Atlanta	New York City	Miami
Social	0.0056 (random)	0.35** (clustered)	0.10* (clustered)	0.10** (clustered)	0.21 ** (clustered)	0.18** (clustered)
Ecological	−0.011 (random)	0.53** (clustered)	0.16** (clustered)	0.33** (clustered)	0.20** (clustered)	0.15** (clustered)
Technological	0.78** (clustered)	0.041** (clustered)	0.44** (clustered)	0.0022* (clustered)	0.87** (clustered)	0.0053 (random)

* Statistically significant at the 0.05 level.
** Statistically significant at the 0.01 level.

Table 5
Correlation coefficient between S-E, S-T, and E-T vulnerability categories in each city.

Vulnerability Domains	Portland (n = 58)	Phoenix (n = 966)	Baltimore (n = 133)	Atlanta (n = 305)	New York City (n = 2361)	Miami (n = 297)
S-E	−0.034	0.097**	0.118	0.227**	0.027	−0.049
S–T	0.420**	−0.006	0.017	−0.012	0.087**	−0.022
E–T	0.033	0.053	0.245**	−0.075	0.052*	−0.017

** Correlation is statistically significant at the 0.01 level.
* Significant at the 0.05 level.

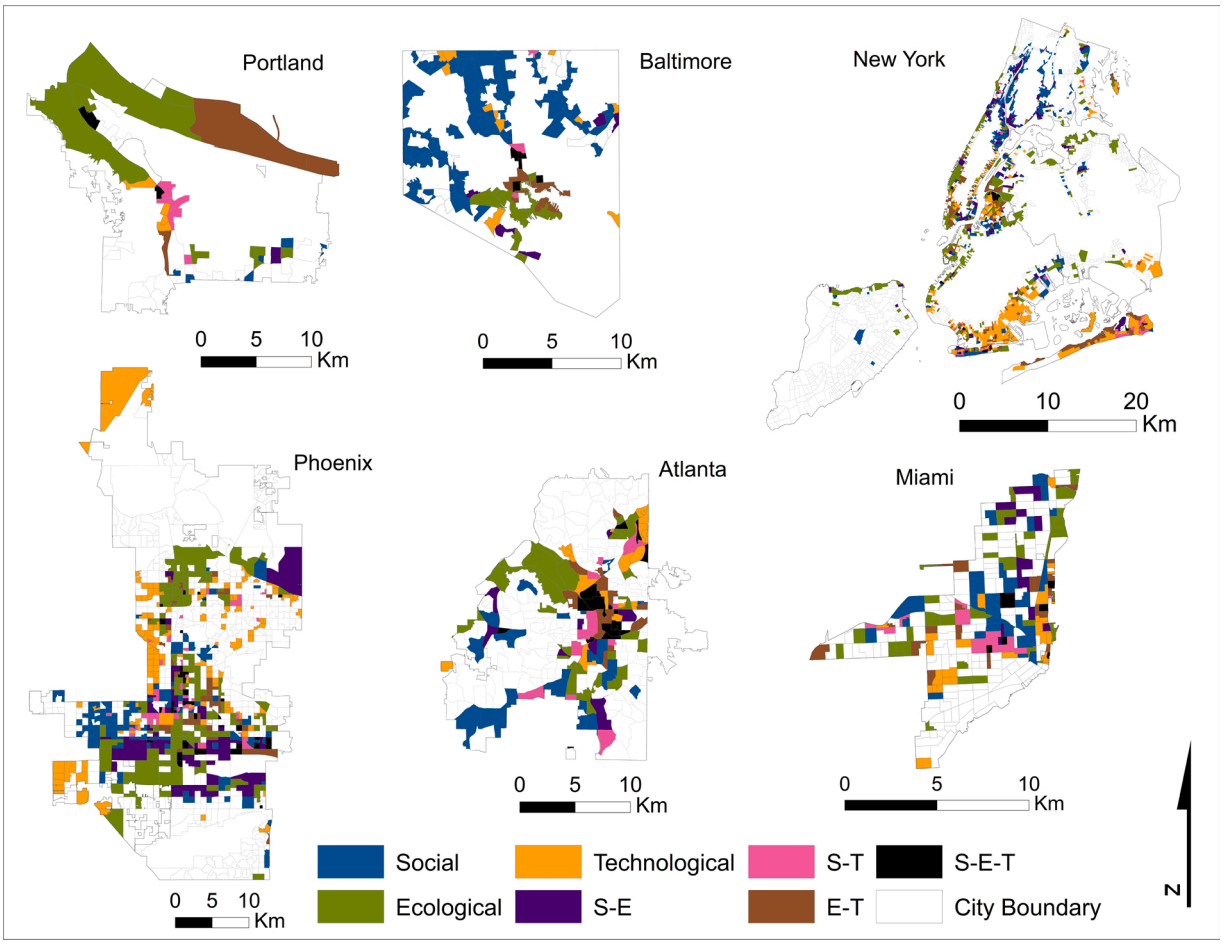

Fig. 6. Combined top-quartile social (S), ecological (E), and technological (T) vulnerability to flooding for six US cities.

correlated to each other. However, the intersecting S- E-T flood vulnerable areas are located along the edge of Wynwood intersected by I-95. Other famous tourist locations like areas of Little Havana and the Omni neighborhood also emerge as having intersecting S- E-T urban flood vulnerability. The predominant spatial patterns are in single domains of social, ecological, and technological vulnerability, with some clustered (although not significant) S-T south along the Miami River in areas of the West Flagler, Little Havana, and Riverside neighborhoods.

4.7. Cross-city comparison

According to the principal component analysis (PCA) results, the first six components explained approximately 60 % of the variation in the vulnerability data across all cities (Table 6). The first two components (components 1 and 2) represent a combination of social, ecological, and technological domains, and explained 26 % of variation. The other components represent ecological and technological elements (components 3 and 6) and social (component 4) and technological elements (component 5). While most indicators were included in a specific component once, building density and street density indicators were included twice in different components, suggesting that built environmental characteristics are important for understanding urban flood vulnerability. When these six components were used in stepwise regression analysis, 44 % of the combined S- E-T flood vulnerability variation was explained by the six components. All but component 4 were positively related to the combined S- E-T flood variability. The first two components, which include all S, E, and T indicators, were statistically the most significant.

5. Discussion

5.1. Importance of considering SETS domains in urban flood vulnerability analysis

The urban SETS flood vulnerability framework developed in this study advances a systematic approach to understanding urban

Table 6
Principal components and selected vulnerability indicators in each component and associated vulnerability domains.

PCA component	Selected indicators (numbers in parenthesis show correlation coefficient*)	Variation explained by this component
Component 1 (S- E-T)	Population (0.58), Age>65 (-0.85), slope sd (0.70), productivity (0.70), street density (-0.62),	14.91 %
Component 2 (S- E-T)	Population density (0.75), wetland (-0.43), building density (0.80), impervious surface (0.62)	11.53 %
Component 3 (E-T)	SI-patch index (-0.62), street density (0.41), impervious surface (-0.53), GI density (0.60)	10.69 %
Component 4 (S)	English (-0.65), income (0.81), renter (0.65)	9.95 %
Component 5 (T)	Distance to emergency (0.82)	6.77 %
Component 6 (E-T)	Bare soil (0.46), critical infrastructure (0.85)	6.43 %

* Correlation coefficient higher than 0.4 was selected for inclusion.

vulnerability to flooding. Many previous flood vulnerability studies have focused on respective SETS domains, yet recognize a need for integrated vulnerability assessments across these domains. For social vulnerability, for example (e.g., Cutter et al., 2003), a growing body of literature in recent years addresses the importance of integrating physical and institutional aspects of vulnerability (e.g., Cho & Chang, 2017). Moreover, only a few studies have explicitly investigated flood vulnerability in the ecological domain. Our results indicate the importance of considering ecological indicators; in this case, productivity and wetlands are included in the first two PCA components. Thus, our study extends earlier endeavors by embracing the neglected ecological aspect of urban flood vulnerability assessment. While nature-based solutions, such as green infrastructure and restored wetlands, are gaining popularity in cities worldwide (Chan et al., 2018; Frantzeskaki et al., 2019; Keeler et al., 2019; Ruangpan et al., 2020), such efforts have not been widely incorporated into analyses of urban flood vulnerability to date, except for a few studies that examined the effectiveness of green infrastructure in flood mitigation (e.g., Fahy & Chang, 2019). Similarly, many technological vulnerability studies typically have not included social and ecological domains (Kim et al., 2017).

5.2. Spatialization of urban flood vulnerability

As one of the few studies examining flood vulnerability across multiple cities and multiple elements, the current study illuminates the multifaceted domains of flood vulnerability at a finer spatial scale. Within the 500-year floodplain, there are substantial spatial variations in social, ecological, and technological domains of vulnerability. This spatial heterogeneity of flood vulnerability suggests that hazardscapes (i.e., the spatial distribution of risk and vulnerability) could be deeply rooted in historical land development (Chang et al., 2021), past discriminatory practices such as redlining (Grove, Cox, & Barnett, 2020), and inappropriate zoning or lack of zoning in some cities. For example, in Phoenix, Baltimore, and Atlanta, the development of housing and infrastructure are not spatially random, and in many instances, these incompatible land uses are co-located in low-income or minority neighborhoods, to the detriment of these socially vulnerable groups. Exploring historical land-use and demographic information about today's vulnerable spaces often reveals legacies of past injustice. The legacy of past discrimination against minority populations, where restrictions and redlining happened, resulted in the concentration of low-income, non-English-speaking populations in specific areas of our study cities (Bolin, Grineski, & Collins, 2005; Grove et al., 2018, 2020; York et al., 2014), as highways and low-income and high renter neighborhoods are co-located. Additionally, the siting of polluting industry (as measured by proximity to TRI sites) near rivers and coastlines contributes to high ecological and social vulnerability in some neighborhoods in Miami, New York City, and Portland. Our findings agree with other studies that identified spatial inequity with respect to the exposure of certain groups of residents (e.g., economically disadvantaged groups) residing in flood-prone zones (La Rosa & Pappalardo, 2020; Qiang, 2019).

5.3. Implications for flood resilience planning

The urban SETS flood vulnerability framework provides useful framing and information for flood resilience planning, design, and policy. Our analyses reveal interactions among the three domains (S, E, and T) along three dimensions (exposure, sensitivity, and adaptive capacity) of vulnerability in each city. With limited resources and capacity to address flood vulnerability, cities may seek to identify neighborhoods with overlapping areas of high S, E, and T vulnerability (as revealed by our quartile S- E-T maps), rather than to reduce vulnerability in only one domain. Alternatively, a city can target specific types of solutions to reduce S, E, T, S-E, or S-T exposure and increase adaptive capacity (Iwaniec, Cook, Davidson, Berbés-Blázquez, & Grimm, 2020). For example, reducing exposure in one domain (e.g., high concentration of people along coastlines), combined with increasing adaptive capacity in another (e.g., expansion of wetlands), may serve as a way to increase resilience and reduce vulnerability, using all domains of the urban SETS vulnerability framework. Correlation results show that in some cities, for example, Atlanta and Phoenix, social and ecological vulnerabilities are significantly related, suggesting that these cities have opportunities to improve neighborhoods that are both socially and ecologically vulnerable. In this regard, city planners might develop green spaces with a focus on equitable distribution throughout the city, and with the intention of increasing social capital to enhance adaptive capacity in poorer neighborhoods. Knowing that social vulnerability is co-located with ecologically vulnerable areas can help city planners promote social protections against displacement of low-income residents for planning ecological improvements in consideration of social and environmental equity. For example, ecological investments in high S-E vulnerability areas might be accompanied by affordable housing policies and meaningful engagement of residents in decision-making and siting, to avoid gentrification and displacement (Cheng, 2019a, b, Foster et al., 2019).

The methods and framework used in the current study are transferable to other types of hazards such as heat that, like flooding, have spatially defined SETS domains (Fahy et al., 2019). As cities are experiencing more cascading hazards with combinations of more than one extreme event, the urban SETS vulnerability framework can offer a useful decision tool for disaster experts and city practitioners.

5.4. Limitations of the current approach and future research suggestions

We developed representative indicators for assessing flood vulnerability across six study cities based on previous practice and a new urban SETS flood vulnerability framework, subject to data availability for all cities that has the advantage of compatibility among the cities. Yet, this study is not intended to be a comprehensive or definitive guide to urban SETS flood vulnerability analysis. Rather, we hope it will serve as a palimpsest on which further exploration of SETS vulnerability can be done, with an expanded set of variables or with more regional specificity, as future researchers see fit. We acknowledge that vulnerability indicators should be further developed with the consultation and engagement of city practitioners and other stakeholders, and that the resulting distributions of SETS vulnerability to flooding or other hazards

may vary greatly, depending on what indicators are considered for analysis. Each city faces unique opportunities and challenges in using specific indicators, which should be considered when updating flood vulnerability maps. For example, measures of ecosystem productivity relying on greenness metrics such as NDVI may be less appropriate for arid-land cities like Phoenix than they are for cities with high canopy cover, such as Portland or Baltimore. Additionally, we applied the framework using an equal weight for all vulnerability indicators. Given that some specific indicators might be more influential than others in a specific regional context (Papathoma-Köhle, Cristofari, Wenk, & Fuchs, 2019), future research could consider conducting stakeholder interviews or surveys to identify their subjective ranking on indicators (Luke et al., 2018). To incorporate stakeholders' perspectives into flood vulnerability analysis, one can use multicriteria decision making, such as the analytical hierarchy process (Hong & Chang, 2020; Ouma & Tateishi, 2014).

The current analysis, which employed widely available existing flood exposure maps, has limitations for assessing future flood vulnerability. As climate change is likely to increase the frequency of extreme weather events and thus the occurrence and distribution of floods (Kundzewicz et al., 2013; Wing et al., 2018), the analysis points to the need for updates using the latest climate-change projections and hydrologic modeling. Additionally, our study addresses only fluvial (riverine) flooding, not including pluvial flooding, which may become more prevalent with the changing climate (Rosenzweig et al., 2018). The flood-prone areas beyond the 500-year floodplain are excluded in our analysis, except for Atlanta, Phoenix, and Miami, where their 500-year floodplains encompass all city areas. Future research can take advantage of the output maps derived from combined modeling of fluvial and pluvial flooding, such as those used in Japan (Tanaka, Kiyohara, & Tachikawa, 2020), in the UK (Muthusamy, Rivas Casado, Salmoral, Irvine, & Leinster, 2019), and in the US (Zhang, Ye, & Yu, 2020).

6. Conclusions

This study reveals the value of using the SETS framework for evaluating flood vulnerability at the census block group scale across six US cities. First, vulnerability to flooding in each SETS domain exhibits a clustered distribution in most cities. We observed unique hotspots of social, ecological, or technological vulnerability, suggesting that the SETS framework offers complementary views for understanding urban vulnerability to flooding across cities. Second, S-E, S-T, and E-T vulnerability are spatially correlated to each other in some cities, suggesting that these cities have opportunities to improve flood mitigation in more than one domain simultaneously. Third, when all 18 indicators are used to explain the combined S- E-T vulnerability, six PCA components explain 44 % of the variance in flood vulnerability across all six cities. The first two components contain indicators that represent all domains of SETS, indicating that failure to consider all three SETS domains in terms of the three dimensions of vulnerability (exposure, sensitivity, and adaptive capacity) will lead to underestimation of system vulnerability.

The findings of this study offer several implications for cities undertaking spatial planning for climate resilience and sustainable development. As indicated earlier, S, E, and T are integrated with exposure, sensitivity and adaptability which is an important contribution to urban sustainability and its societal dimensions. The relevance to cities is underscored by the application to six U.S. cities and other cities can benefit from these findings. An understanding of complex, interconnected components is critical to an understanding of sustainable development. SETS provides a framework to examine the complex relationship between environment, infrastructure, and equitable distribution of hazards in society. Because areas that are vulnerable to floods are spatially confined to specific areas, municipalities can target the neighborhoods in which hotspots (top 25 % of vulnerability scores) of more than one SETS domain overlap. If a neighborhood lacks green space or contains infrastructure that makes it vulnerable to floods, cities can invest in such neighborhoods to improve existing conditions, while also improving social resilience. Additionally, the urban SETS flood vulnerability framework can be further refined with local stakeholders' explicit engagement, including community members, by adding or subtracting indicators and assigning weights. As the flood resilience agenda of community members might differ from that of city practitioners or other experts (Grove et al., 2020), it is essential to hear different voices and incorporate these diverse perspectives into future resilience planning. The urban SETS flood vulnerability framework offers a platform for engaging diverse stakeholders to co-produce knowledge to achieve flood resilience under changing demographics and climate to ensure the sustainability of equitable economic investment on infrastructure and technological systems to reduce flooding vulnerability and enhance resilience in ecosystems and communities.

Declaration of Competing Interest

The authors declare that they have no known competing financial interests or personal relationships that could have appeared to influence the work reported in this paper.

Acknowledgments

This material is based upon work supported by the National Science Foundation under Award Numbers (SES cooperative agreement 1444755, 1832016, 1934933, 1927468, and 1927167). We appreciate city practitioners who graciously shared the GIS data used for analysis. Thank you also to those who reviewed the initial version of the manuscript and offered useful feedback at the Virtual All Hands workshop in April 2020.

References

Adelekan, I. O. (2011). Vulnerability assessment of an urban flood in Nigeria: Abeokuta flood 2007. *Natural Hazards, 56*(1), 215–231. https://doi.org/10.1007/s11069-010-9564-z

American Rivers, 2020. https://www.americanrivers.org/rivers/discover-your-river/10-facts-about-flooding/#:~:text=Damages%20from%20flood%20losses%20have%20increased%20to%20an%20average%20%2410%20billion%20per%20year (Assessed on July 26, 2020).

Askins, R. A. (1995). Hostile landscapes and the decline of migratory songbirds. *Science, 267*(5206), 1956–1957. https://doi.org/10.1126/science.267.5206.1956

ASFPM (Association of State Floodplain Managers). (2020). *A cost analysis for completing and maintaining the Nation's NFIP flood map inventory*. Madison: WI.

Bevers, M., & Flather, C. H. (1999). Numerically exploring habitat fragmentation effects on populations using cell-based coupled map lattices. *Theoretical Population Biology, 55*(1), 61–76. https://doi.org/10.1006/tpbi.1998.1392

Blessing, R., Sebastian, A., & Brody, S. D. (2017). Flood risk delineation in the United States: How much loss are we capturing? *Natural Hazards Review, 18*(3). https://doi.org/10.1061/(ASCE)NH.1527-6996.0000242, 04017002.

Bolin, B., Grineski, S., & Collins, T. (2005). The geography of despair: Environmental racism and the making of South Phoenix, Arizona, USA. *Human Ecology Review, 12*, 156–168.

Borden, K. A., Schmidtlein, M. C., Emrich, C. T., Piegorsch, W. W., & Cutter, S. L. (2007). Vulnerability of U.S. cities to environmental hazards. *Journal of Homeland Security and Emergency Management, 4*(2). https://doi.org/10.2202/1547-7355.1279

Chakraborty, J., Grineski, S. E., & Collins, T. W. (2019). Hurricane Harvey and people with disabilities: Disproportionate exposure to flooding in Houston, Texas. *Social Science & Medicine, 226*, 176–181. https://doi.org/10.1016/j.socscimed.2019.02.039

Chan, F. K., Griffiths, J. A., Higgitt, D., Xu, S., Zhu, F., Tang, Y., & Thorne, C. R. (2018). "Sponge City" in China—A breakthrough of planning and flood risk management in the urban context. *Land Use Policy, 76*, 772–778. https://doi.org/10.1016/j.landusepol.2018.03.005

Chang, H., Yu, D., Markolf, S., Hong, C., Eom, S., Song, W., … Bae, D. (2021). Understanding urban flood resilience in the anthropocene: A social-ecological-technological systems (SETS) learning framework. *Annals of the American Association of Geographers*. https://doi.org/10.1080/24694452.2020.1850230

Cheng, C. (2019a). EcoWisdom for climate justice planning: Social-ecological vulnerability assessment in Boston's Charles River watershed. *EcoWISE Ecological Wisdom*, 249–265. https://doi.org/10.1007/978-981-13-0571-9_13

Cheng, C. (2019b). Climate justicescape and implications for urban resilience in American cities. In M. Burayidi, J. Twigg, A. Allen, & C. Wamlester (Eds.), *The routledge handbook of urban resilience* (pp. 83–96). New York, NY: Routledge, Taylor & Francis Books.

Cheng, C., Yang, E. Y.-C., Ryan, R. L., Yu, Q., & Brabec, E. (2017). Assessing climate change-induced flooding mitigation for adaptation in Boston's Charles River Watershed. *Landscape and Urban Planning, 167*, 25–36. https://doi.org/10.1016/j.landurbplan.2017.05.019

Childers, D. L., Bois, P., Hartnett, H. E., McPhearson, T., Metson, G. S., & Sanchez, C. A. (2019). Urban ecological infrastructure: An inclusive concept for the non-built urban environment. *Elementa: Science of the Anthropocene, 7*, 46. https://doi.org/10.1525/elementa.385

Cho, S., & Chang, H. (2017). Recent research approaches to Urban flood vulnerability, 2006-2016. *Natural Hazards, 88*(1), 633–649. https://doi.org/10.1007/s11069-017-2869-4

Collins, T. W., Grineski, S. E., Chakraborty, J., & Flores, A. B. (2019). Environmental injustice and Hurricane Harvey: A household-level study of socially disparate flood exposures in Greater Houston, Texas, USA. *Environmental Research, 179*, Article 108772. https://doi.org/10.1016/j.envres.2019.108772

Cook, E. M., Berbés-Blázquez, M., Grimm, N. B., Iwaniec, D. M., Mannetti, L., Muñoz-Erickson, T. A., et al. (2021). Setting the stage for meaningful co-production. In Z. Hamstead (Ed.), *Resilient urban futures* (pp. 95–107). Springer-Nature, 95-107.

Cooley, A., & Chang, H. (2020). Detecting change in precipitation indices using observed (1977-2016) and modeled future climate data in Portland, Oregon, USA. *Journal of Water and Climate Change*. https://doi.org/10.2166/wcc.2020.043

Cutter, S. L. (2016). *Social vulnerability and Community resilience measurement and tools*. University of South Carolina, HVRI.

Cutter, S. L., Boruff, B. J., & Shirley, W. L. (2003). Social vulnerability to environmental hazards. *Social Science Quarterly, 84*, 242–261. https://doi.org/10.1111/1540-6237.8402002

Danielson, T. M., Rivera-Monroy, V. H., Castañeda-Moya, E., Briceño, H., Travieso, R., Marx, B. D., Gaiser, E., & Farfán, L. M. (2017). Assessment of everglades mangrove forest resilience: Implications for above-ground net primary productivity and carbon dynamics. *Forest Ecology and Management, 404*, 115–125. https://doi.org/10.1016/j.foreco.2017.08.009

Environmental Systems Research Institute (ESRI). ArcGIS Desktop: Release 10.7, 2020. Redlands, CA: Environmental Systems Research Institute.

Erena, S. H., & Worku, H. (2019). Urban flood vulnerability assessments: The case of Dire Dawa city, Ethiopia. *Natural Hazards, 97*(2), 495–516. https://doi.org/10.1007/s11069-019-03654-9

Ewers, R. M., & Didham, R. K. (2007). The effect of fragment shape and species' sensitivity to habitat edges on animal population size. *Conservation Biology, 21*(4), 926–936. https://doi.org/10.1111/j.1523-1739.2007.00720.x

Fahy, B., & Chang, H. (2019). Effects of stormwater green infrastructure on watershed outflow: Does spatial distribution matter? *International Journal of Geospatial and Environmental Research, 6*(1). https://dc.uwm.edu/ijger/vol6/iss1/5/.

Fahy, B., Brenneman, E., Chang, H., & Shandas, V. (2019). Spatial analysis of urban floods and extreme heat potential in Portland, OR. *International Journal of Disaster Risk Reduction, 39*, 101117. https://doi.org/10.1016/j.ijdrr.2019.101117

FEMA. (2020). *From FEMA flood service map center. Search all products website*. Retrieved Mar 22, 2020 https://msc.fema.gov/portal/availabilitySearchz.

Ferrari, S., Oliveira, S., Pautasso, G., & Zêzere, J. L. (2019). Territorial resilience and flood vulnerability. Case studies at Urban scale in Torino (Italy) and Porto/Vila Nova de Gaia (Portugal). *Resilient cities urban resilience for risk and adaptation governance* (pp. 147–174). https://doi.org/10.1007/978-3-319-76944-8_10

Foster, S., Leichenko, R., Nguyen, K. H., Blake, R., Kunreuther, H., Madajewicz, M., Petkova, E. P., Zimmerman, R., Corbin-Mark, C., Yeampierre, E., Tovar, A., Herrara, C., & Ravenborg, D. (2019). "Chapter 6: Community-Based assessments of adaptation and equity," in: New York City Panel on Climate Change (NPCC), advancing tools and methods for flexible adaptation pathways and science policy integration: NPCC 2019 report. In C. Rosenzweig, & W. Solecki (Eds.), *Annals of the New York academy of sciences, 1439, March 15* (pp. 126–1439173). https://doi.org/10.1111/nyas.14009

Frantzeskaki, N., Mcphearson, T., Collier, M. J., Kendal, D., Bulkeley, H., Dumitru, A., & Pintér, L. (2019). Nature-based solutions for urban climate change adaptation: Linking science, policy, and practice communities for evidence-based decision-making. *BioScience, 69*(6), 455–466. https://doi.org/10.1093/biosci/biz042

Gimenez-Maranges, M., Pappalardo, V., La Rosa, D., Breuste, J., & Hof, A. (2020). The transition to adaptive storm-water management: Learning from existing experiences in Italy and Southern France. *Sustainable Cities and Society, 55*, 102061. https://doi.org/10.1016/j.scs.2020.102061

Grimm, N. B., Pickett, S. T. A., Hale, R. L., & Cadenasso, M. L. (2017). Does the ecological concept of disturbance have utility in urban social-ecological-technological systems? *Ecosystem Health and Sustainability, 3*(1). https://doi.org/10.1002/ehs2.1255

Grove, M., Ogden, L., Pickett, S., Boone, C., Buckley, G., Locke, D. H., … Hall, B. (2018). The legacy effect: Understanding how segregation and environmental injustice unfold over time in Baltimore. *Annals of the American Association of Geographers, 108*(2), 524–537. https://doi.org/10.1080/24694452.2017.1365585

Grove, K., Cox, S., & Barnett, A. (2020). Racializing resilience: Assemblage, critique, and contested futures in Greater Miami resilience planning. *Annals of the American Association of Geographers, 110*(5), 1613–1630. https://doi.org/10.1080/24694452.2020.1715778

Gu, H., Du, S., Liao, B., Wen, J., Wang, C., Chen, R., … Chen, B. (2018). A hierarchical pattern of urban social vulnerability in Shanghai, China and its implications for risk management. *Sustainable cities and society, 41*, 170–179. https://doi.org/10.1016/j.scs.2018.05.047

Guidotti, R., Chmielewski, H., Unnikrishnan, V., Gardoni, P., Mcallister, T., & Lindt, J. V. (2016). Modeling the resilience of critical infrastructure: The role of network dependencies. *Sustainable and Resilient Infrastructure, 1*(3-4), 153–168. https://doi.org/10.1080/23789689.2016.1254999

Han, Y., Huang, Q., He, C., Fang, Y., Wen, J., Gao, J., … Du, S. (2020). The growth mode of built-up land in floodplains and its impacts on flood vulnerability. *Science of The Total Environment, 700*, 134462. https://doi.org/10.1016/j.scitotenv.2019.134462

Highfield, W. E., Norman, S. A., & Brody, S. D. (2013). Examining the 100-year floodplain as a metric of risk, loss, and household adjustment. *Risk Analysis: An International Journal, 33*(2), 186–191. https://doi.org/10.1111/j.1539-6924.2012.01840.x

Hong, C-y., & Chang, H. (2020). Residents' perception of flood risk and urban stream restoration using multi-criteria decision analysis. *River research and applications*. https://doi.org/10.1002/rra.3728

Iwaniec, D. M., Cook, E. M., Davidson, M. J., Berbés-Blázquez, M., Georgescu, M., Krayenhoff, E. S., … Grimm, N. B. (2020). The co-production of sustainable future scenarios. *Landscape and Urban Planning, 197*, 103744. https://doi.org/10.1016/j.landurbplan.2020.103744

Iwaniec, D. M., Cook, E. M., Davidson, M. J., Berbés-Blázquez, M., & Grimm, N. B. (2020). Integrating existing climate adaptation planning into future visions: A strategic scenario for the central Arizona–Phoenix region. *Landscape and Urban Planning, 200*, 103820. https://doi.org/10.1016/j.landurbplan.2020.103820

Iyengar, N. S., & Sudarshan, P. (1982). A method of classifying regions from multivariate data. *Economic and Political Weekly, 17*, 2048–2052.

Janssen, E., Wuebbles, D. J., Kunkel, K. E., Olsen, S. C., & Goodman, A. (2014). Observational- and model-based trends and projections of extreme precipitation over the contiguous United States. *Earth's Future, 2*(2), 99–113. https://doi.org/10.1002/2013ef000185

Jolliffe, I. T. (2002). *Principal component analysis* (second edition). NY: Springer-Verlag.

Kaiser, H. F. (1958). The varimax criterion for analytic rotation in factor analysis. *Psychometrika, 23*(3), 187–200. https://doi.org/10.1007/BF02289233

Kasperson, J. X. & Kasperson, R. E. SEI Risk and Vulnerability Programme Report 2001-01, 2001, Stockholm Environment Institute, Stockholm.

Keeler, B. L., Hamel, P., Mcphearson, T., Hamann, M. H., Donahue, M. L., Prado, K. A., & Wood, S. A. (2019). Social-ecological and technological factors moderate the value of urban nature. *Nature Sustainability, 2*(1), 29–38. https://doi.org/10.1038/s41893-018-0202-1

Khajehei, S., Ahmadalipour, A., Shao, W., & Moradkhani, H. (2020). A Place-based assessment of flash flood hazard and vulnerability in the contiguous United States. *Scientific Reports, 10*(1). https://doi.org/10.1038/s41598-019-57349-z

Kiaghadi, A., & Rifai, H. S. (2019). Physical, chemical, and microbial quality of floodwaters in Houston following hurricane Harvey. *Environmental Science & Technology, 53*(9), 4832–4840. https://doi.org/10.1021/acs.est.9b00792

Kim, Y., Eisenberg, D. A., Bondank, E. N., et al. (2017). Fail-safe and safe-to-fail adaptation: Decision-making for urban flooding under climate change. *Climatic Change, 145*, 397–412. https://doi.org/10.1007/s10584-017-20901

Kirby, R. H., Reams, M. A., Lam, N. S., Zou, L., Dekker, G. G., & Fundter, D. Q. P. (2019). Assessing social vulnerability to flood hazards in the Dutch Province of Zeeland. *International Journal of Disaster Risk Science, 10*(2), 233–243. https://doi.org/10.1007/s13753-019-0222-0

Kundzewicz, Z. W., Kanae, S., Seneviratne, S. I., Handmer, J., Nicholls, N., Peduzzi, P., & Sherstyukov, B. (2018). Flood risk and climate change: Global and regional perspectives. *Hydrological Sciences Journal, 59*(1), 1–28. https://doi.org/10.1080/02626667.2013.857411

Kunkel, K. E., Karl, T. R., Squires, M. F., Yin, X., Stegall, S. T., & Easterling, D. R. (2020). Precipitation extremes: Trends and relationships with average precipitation and precipitable Water in the contiguous United States. *Journal of Applied Meteorology and Climatology, 59*(1), 125–142. https://doi.org/10.1175/jamc-d-19-0185.1

La Rosa, D., & Pappalardo, V. (2020). Planning for spatial equity-a performance based approach for sustainable urban drainage systems. *Sustainable Cities and Society, 53*, 101885. https://doi.org/10.1016/j.scs.2019.101885

Laudan, J., Rözer, V., Sieg, T., Vogel, K., & Thieken, A. H. (2017). Damage assessment in Braunsbach 2016: Data collection and analysis for an improved understanding of damaging processes during flash floods. *Natural Hazards and Earth System Sciences, 17*(12), 2163–2179. https://doi.org/10.5194/nhess-17-2163-2017

Luke, A., Sanders, B. F., Goodrich, K. A., Feldman, D. L., Boudreau, D., Eguiarte, A., Serrano, K., Reyes, A., Schubert, J. E., AghaKouchak, A., & Basolo, V. (2018). Going beyond the flood insurance rate map: Insights from flood hazard map co-production. *Natural Hazards and Earth System Sciences, 18*(4). https://doi.org/10.5194/nhess-18-1097-2018, 2018.

Ma, C., & Smith, T. (2020). Vulnerability of renters and Low-income households to storm damage: Evidence from hurricane Maria in Puerto Rico. *American Journal of Public Health, 110*(2), 196–202. https://doi.org/10.2105/ajph.2019.305438

Manturuk, K., Lindblad, M., & Quercia, R. (2010). Friends and neighbors: Homeownership and social capital among low- to moderate-income families. *Journal of Urban Affairs, 32*(4), 471–488. https://doi.org/10.1111/j.1467-9906.2010.00494.x

Markolf, S., Chester, M., Eisenberg, D., Iwaniec, D., Ruddell, B., Davidson, C., Zimmerman, R., Miller, T., & Chang, H. (2018). Interdependent Infrastructure as Linked Social, Ecological, and Technological Systems (SETS) to Address Lock-In and Improve Resilience. *Earth's Future, 6*(12), 1638–1659. https://doi.org/10.1029/2018EF000926

McCarthy, J. J., Canziani, O. F., Leary, N. A., Dokken, D. J., & White, K. S. (2001). *Climate Change 2001: Impacts, adaptation, and vulnerability. Contribution of working group II to the third assessment report of the intergovernmental panel on climate change*. Cambridge, UK; New York, NY, USA: Cambridge University Press.

Martínez-Morales, M. A. (2005). Landscape patterns influencing bird assemblages in a fragmented neotropical cloud forest. *Biological Conservation, 121*(1), 117–126. https://doi.org/10.1016/j.biocon.2004.04.015

McPhearson, T., Pickett, S. T. A., Grimm, N. B., Niemelä, J., Alberti, M., Elmqvist, T., Weber, C., Haase, D., Breuste, J., & Qureshi, S. (2016). Advancing urban ecology toward a science of cities. *Bioscience, 66*(3), 198–212. https://doi.org/10.1093/biosci/biw002

Mohtar, W. H., Abdullah, J., Maulud, K. N., & Muhammad, N. S. (2020). Urban flash flood index based on historical rainfall events. *Sustainable Cities and Society, 56*, 102088. https://doi.org/10.1016/j.scs.2020.102088

Moran, P. A. P. (1950). Notes on continuous stochastic phenomena. *Biometrika, 37*(1), 17–23. https://doi.org/10.2307/2332142

Müller, A., Reiter, J., & Weiland, U. (2011). Assessment of urban vulnerability towards floods using an indicator-based approach – A case study for Santiago de Chile. *Natural Hazards and Earth System Sciences, 11*(8), 2107–2123. https://doi.org/10.5194/nhess-11-2107-2011

Muñoz-Erickson, T. A., Miller, C. A., & Miller, T. R. (2017). How cities think: Knowledge co-production for urban sustainability and resilience. *Forests, Trees and Livelihoods, 8*(6), 203. https://doi.org/10.3390/f8060203

Muthusamy, M., Rivas Casado, M., Salmoral, G., Irvine, T., & Leinster, P. (2019). A remote sensing based integrated approach to quantify the impact of fluvial and pluvial flooding in an urban catchment. *Remote Sensing, 11*(5), 577. https://doi.org/10.3390/rs11050577

Nasiri, H., Yusof, M. J., & Ali, T. A. (2016). An overview to flood vulnerability assessment methods. *Sustainable Water Resources Management, 2*(3), 331–336. https://doi.org/10.1007/s40899-016-0051-x

Nasiri, H., Yusof, M. J., Ali, T. A., & Hussein, M. K. (2019). District flood vulnerability index: Urban decision-making tool. *International Journal of Environmental Science and Technology, 16*(5), 2249–2258. https://doi.org/10.1007/s13762-018-1797-5

OECD. (2016). *Financial management of food risk*. Available at https://www.oecd.org/finance/financial-management-of-flood-risk.htm.

Ouma, Y., & Tateishi, R. (2014). Urban flood vulnerability and risk mapping using integrated multi-parametric AHP and GIS: Methodological overview and case study assessment. *Water, 6*(6), 1515–1545. https://doi.org/10.3390/w6061515

Palla, A., & Gnecco, I. (2015). Hydrologic modeling of Low impact development systems at the urban catchment scale. *Journal of Hydrology, 528*, 361–368. https://doi.org/10.1016/j.jhydrol.2015.06.050. Elsevier B.V.

Papathoma-Köhle, M., Cristofari, G., Wenk, M., & Fuchs, S. (2019). The importance of indicator weights for vulnerability indices and implications for decision making in disaster management. *International Journal of Disaster Risk Reduction, 36*, 101103. https://doi.org/10.1016/j.ijdrr.2019.101103

Polsky, C., Neff, R., & Yarnal, B. (2007). Building comparable global change vulnerability assessments: The vulnerability scoping diagram. *Global Environmental Change, 17*(3-4), 472–485. https://doi.org/10.1016/j.gloenvcha.2007.01.005

Pratt, B., & Chang, H. (2012). Effects of land cover, topography, and built structure on seasonal water quality at multiple spatial scales. *Journal of Hazardous Materials, 209-210*, 48–58. https://doi.org/10.1016/j.jhazmat.2011.12.068

Pregnolato, M., Ford, A., Glenis, V., Wilkinson, S., & Dawson, R. (2017). Impact of climate change on disruption to urban transport networks from pluvial flooding. *Journal of Infrastructure Systems, 23*(4), 04017015. https://doi.org/10.1061/(asce)is.1943-555x.0000372

Qiang, Y. (2019). Disparities of population exposed to flood hazards in the United States. *Journal of Environmental Management, 232*(15). https://doi.org/10.1016/j.jenvman.2018.11.039

Qiang, Y., Lam, N. S., Cai, H., & Zou, L. (2017). Changes in exposure to flood hazards in the United States. *Annals of the American Association of Geographers, 107*(6), 1332–1350. https://doi.org/10.1080/24694452.2017.1320214

Römer, H., Willroth, P., Kaiser, G., Vafeidis, A. T., Ludwig, R., Sterr, H., … Diez, J. R. (2012). Potential of remote sensing techniques for tsunami hazard and vulnerability analysis – A case study from Phang-Nga province, Thailand. *Natural Hazards and Earth System Sciences, 12*(6), 2103–2126. https://doi.org/10.5194/nhess-12-2103-2012

Rosenzweig, B. R., McPhillips, L., Chang, H., Cheng, C., Welty, C., Matsler, M., … Davidson, C. (2018). *Urban pluvial flood risk and opportunities for resilience* (p. e1302). WIREs. https://doi.org/10.1002/wat2.1302

Ruangpan, L., Vojinovic, Z., Sabatino, S. D., Leo, L. S., Capobianco, V., Oen, A. M., … Lopez-Gunn, E. (2020). Nature-based solutions for hydro-meteorological risk reduction: A state-of-the-art review of the research area. *Natural Hazards and Earth System Sciences, 20*(1), 243–270. https://doi.org/10.5194/nhess-2019-128-rc2

Rufat, S., Tate, E., Burton, C. G., & Maroof, A. S. (2015). Social vulnerability to floods: Review of case studies and implications for measurement. *International Journal of Disaster Risk Reduction, 14*, 470–486. https://doi.org/10.1016/j.ijdrr.2015.09.013

Salazar-Briones, C., Ruiz-Gibert, J. M., Lomelí-Banda, M. A., & Mungaray-Moctezuma, A. (2020). An integrated urban flood vulnerability index for sustainable planning in arid zones of developing countries. *Water, 12*(2), 608. https://doi.org/10.3390/w12020608

Sterzel, T., Lüdeke, M. K., Walther, C., Kok, M. T., Sietz, D., & Lucas, P. L. (2020). Typology of coastal urban vulnerability under rapid urbanization. *Plos One, 15*(1). https://doi.org/10.1371/journal.pone.0220936

Swain, D. L., Wing, O. E. J., Bates, P. D., Done, J. M., Johnson, K. A., & Cameron, D. R. (2020). Increased flood exposure due to climate change and population growth in the United States. *Earth's Future, 8*(11). https://doi.org/10.1029/2020EF001778. e2020EF001778.

Tanaka, T., Kiyohara, K., & Tachikawa, Y. (2020). Comparison of fluvial and pluvial flood risk curves in urban cities derived from a large ensemble climate simulation dataset: A case study in Nagoya, Japan. *Journal of Hydrology, 584*, 124706. https://doi.org/10.1016/j.jhydrol.2020.124706

Turner, B. L., Kasperson, R. E., Matson, P. A., McCarthy, J. J., Corell, R. W., Christensen, L., Eckley, N., Kasperson, J. X., Luers, A., Martello, M. L., & Polsky, C. (2003). A framework for vulnerability analysis in sustainability science. *Proceedings of the national academy of sciences, 100*(14), 8074–8079. https://doi.org/10.1073/pnas.1231335100

UNESCO World Water Assessment Programme. (2012). *United Nations world water development report 4: Managing water under uncertainty and risk*. Available at https://unesdoc.unesco.org/ark:/48223/pf0000215644.page=812.

Veldhuis, J. A., Clemens, F. H., & Gelder, P. H. (2011). Quantitative fault tree analysis for urban water infrastructure flooding. *Structure and Infrastructure Engineering, 7*(11), 809–821. https://doi.org/10.1080/15732470902985876

Weißhuhn, P., Müller, F., & Wiggering, H. (2018). Ecosystem vulnerability review: Proposal of an interdisciplinary ecosystem assessment approach. *Environmental Management, 61*(6), 904–915. https://doi.org/10.1007/s00267-018-1023-8

Wilbanks, T. J., & Fernandez, S. J. (2014). In T. J. Wilbanks, & S. Fernandez (Eds.), *Climate change and infrastructure, urban systems, and vulnerabilities*. Washington, DC: Island Press/Center for Resource Economics. https://doi.org/10.5822/978-1-61091-556-4.

Wilson, B. J., Servais, S., Charles, S. P., Gaiser, E., Kominoski, J. S., Richards, J. H., & Troxler, T. G. (2019). Phosphorus alleviation of salinity stress: effects of saltwater intrusion on an Everglades freshwater peat marsh. *Ecology, 100*(5), e02672. https://doi.org/10.1002/ecy.2672

Wing, O. E., Bates, P. D., Smith, A. M., Sampson, C. C., Johnson, K. A., Fargione, J., … Morefield, P. (2018). Estimates of present and future flood risk in the conterminous United States. *Environmental Research Letters, 13*(3), 034023. https://doi.org/10.1088/1748-9326/aaac65

York, A., Tuccillo, J., Boone, C., Bolin, B., Gentile, L., Schoon, B., … Kane, K. (2014). Zoning and land use: A tale of incompatibility and environmental injustice in early Phoenix. *Journal of Urban Affairs, 36*, 833–853. https://doi.org/10.1111/juaf.12076

Zhang, Y. J., Ye, F., Yu, H., et al. (2020). Simulating compound flooding events in a hurricane. *Ocean Dynamics, 70*, 621–640. https://doi.org/10.1007/s10236-020-01351-x

Zimmerman, R., Restrepo, C. E., Joseph, R. A., & Llopis, J. (2017). A New Role for rail transit: Evacuation. *UTC Spotlight University transportation centers program, #109*. Transportation Research Board. April https://www.transportation.gov/sites/dot.gov/files/docs/utc/April_2017_UTC_Spotlight.pdf.

Zong, Y., & Chen, X. (2000). The 1998 flood on the Yangtze, China. *Natural Hazards, 22*, 165–184.